1. Snover DC, Jass JR, Fenoglio-Preiser C, et al. Serrated polyps of the large intestine. Am J Clin Pathol 2005;124:380–391.
2. Lieberman DA, Moravec M, Holub J, et al. Polyp size and advanced histology in patients undergoing colonoscopy screening: implications for CT colonography. Gastroenterology 2008;135:1100–1105.
3. Winawer SJ, Zauber AG, O'Brien MJ, et al; and the National Polyp Study Workgroup. Randomized comparison of surveillance intervals after colonoscopic removal of newly diagnosed adenomatous polyps. N Engl J Med 1993;328:901–906.
4. Robertson DJ, Greenberg ER, Beach M, et al. Colorectal cancer in patients under close colonoscopic surveillance. Gastroenterology 2005;129:34–41.
5. Lieberman DA, Weiss DG, Harford WV, et al. Five year colon surveillance after screening colonoscopy. Gastroenterology 2007;133:1077–1085.
6. Brenner DJ, Hall EJ. Computed tomography—an increasing source of radiation exposure. N Engl J Med 2007;357:2277–2284.
7. Pickhardt PJ, Hassan C, Laghi A, et al. Clinical management of small (6–9mm) polyps detected at screening CT colonography: a cost-effectiveness analysis. AJR Am J Roentgenol 2008;191:1509–1516.
8. Hur C, Chung DC, Schoen RE, et al. The management of small polyps found by virtual colonoscopy: results of a decision analysis. Clin Gastroenterol Hepatol 2007;5:237–244.
9. Levin B, Lieberman DA, McFarland B, et al. Screening and surveillance for early detection of colorectal cancer and adenomatous polyps, 2008: a joint guideline from the American Cancer Society, the US Multi-Society Task Force on Colorectal Cancer, and the American College of Radiology. Gastroenterology 2008;134:1570–1595.
10. McFarland EG, Levin B, Lieberman DA, et al. Revised colorectal screening guidelines: joint effort of the American Cancer Society U.S. Multisociety Task Force on Colorectal Cancer and American College of Radiology. Radiology 2008;248:717–720.

Correction

Marrache F, Tu SP, Bhagat G, et al. Overexpression of interleukin-1 in the murine pancreas results in chronic pancreatitis. Gastroenterology 2008;135:1277–1287.

In the above article, Dr James M. Masciotti, Department of Biomedical Engineering, Columbia University, New York, New York and Dr Andreas H. Hielscher, Department of Biomedical Engineering and Department of Radiology, Columbia University, New York, New York were inadvertently omitted from the author list.

Dr Frederic Marrache's affiliation at the Department of Gastroenterology, Beaujon Hospital, Paris, France was omitted from the author's affiliation list.

Correction

Cox AL, Page K, Bruneau J, et al. Rare birds in north america: acute hepatitis C cohorts. Gastroenterology 2008;136:26–31.

Incomplete funding was provided at the end of the article. Full funding is cited throughout the text and in Table 1.

BASIC—LIVER, PANCREAS, AND BILIARY TRACT

Overexpression of Interleukin-1β in the Murine Pancreas Results in Chronic Pancreatitis

FREDERIC MARRACHE,* SHUI PING TU,* GOVIND BHAGAT,‡ SWAROOP PENDYALA,§ CHRISTOPH H. ÖSTERREICHER,‖
SHANISHA GORDON,* VIGNESHWARAN RAMANATHAN,* MELITTA PENZ-ÖSTERREICHER,‖ KELLY S. BETZ,*
ZHIGANG SONG,* and TIMOTHY C. WANG*

*Division of Digestive and Liver Diseases, Columbia University Medical Center, New York; ‡Department of Pathology, Columbia University Medical Center, New York;
§Laboratory of Biochemical Genetics and Metabolism, Rockefeller University, New York, New York; and ‖Department of Medicine, University of California San Diego,
La Jolla, California

Background & Aims: Chronic pancreatitis is a significant cause of morbidity and a known risk factor for pancreatic adenocarcinoma. Interleukin-1β is a proinflammatory cytokine involved in pancreatic inflammation. We sought to determine whether targeted overexpression of interleukin-1β in the pancreas could elicit localized inflammatory responses and chronic pancreatitis. **Methods:** We created a transgenic mouse model (elastase sshIL-1β) in which the rat elastase promoter drives the expression of human interleukin-1β. Mice were followed up for up to 2 years. Pancreata of elastase sshIL-1β mice were analyzed for chronic pancreatitis-associated histologic and molecular changes. To study the potential effect of p53 mutation in chronic pancreatitis, elastase sshIL-1β mice were crossed with p53^{R172H} mice. **Results:** Three transgenic lines were generated, and in each line the pancreas was atrophic and occasionally showed dilation of pancreatic and biliary ducts secondary to proximal fibrotic stenosis. Pancreatic histology showed typical features of chronic pancreatitis. There was evidence for increased acinar proliferation and apoptosis, along with prominent expression of tumor necrosis factor-α; chemokine (C-X-C motif) ligand 1; stromal cell-derived factor 1; transforming growth factor-β1; matrix metallopeptidase 2, 7, and 9; inhibitor of metalloproteinase 1; and cyclooxygenase 2. The severity of the lesions correlated well with the level of human interleukin-1β expression. Older mice displayed acinar-ductal metaplasia but did not develop mouse pancreatic intraepithelial neoplasia or tumors. Elastase sshIL-1β*p53$^{R172H/+}$ mice had increased frequency of tubular complexes, some of which were acinar-ductal metaplasia. **Conclusions:** Overexpression of interleukin-1β in the murine pancreas induces chronic pancreatitis. Elastase sshIL-1β mice consistently develop severe chronic pancreatitis and constitute a promising model for studying chronic pancreatitis and its relationship with pancreatic adenocarcinoma.

Chronic pancreatitis leads to a progressive and irreversible destruction of the pancreatic gland.[1] In advanced cases, this may result in pancreatic exocrine insufficiency and/or diabetes. Significant morbidity is also associated with occasional biliary or pancreatic ductal obstruction secondary to fibrotic stenosis or ductal obliteration. Furthermore, chronic pancreatitis is a well-described risk factor for pancreatic adenocarcinoma,[2,3] especially in cases of hereditary chronic pancreatitis.[4]

Although the pathogenesis of the initial pancreatic lesion depends on the etiology of the disease, it is believed that subsequent progression to chronic pancreatitis implies a common mechanism. Two main hypotheses have been proposed. The first one is called the *necrosis-fibrosis sequence* hypothesis and is based on clinical and experimental data, which suggest that chronic pancreatitis could result from repetitive episodes of acute pancreatitis. However, chronic pancreatitis is sometimes observed without evidence of associated necrosis, suggesting a different pathogenic mechanism, also referred to as the *sentinel acute pancreatitis episode* hypothesis. According to the latter, an initial episode of acute pancreatitis elicits chronic inflammation by recruiting immune cells and activating pancreatic stellate cells. Finally, it is possible that both mechanisms occur simultaneously and that their respective contributions vary depending on the etiology of the disease and the presence of additional host or environmental factors.

Several mouse models of chronic pancreatitis have been reported to date, supporting the different aforementioned hypotheses. The most commonly employed model consists of repeated injections of cerulein, an analogue of cholecystokinin, which induces chronic pancreatitis if injected repeatedly over a sufficient period of time, in agreement with the *necrosis-fibrosis sequence* hypothesis.[5] Pancreatic duct ligation is another model that can induce inflammation and pancreatic atrophy.[6] Recently, transgenic mouse models have been developed, some of which are based on genetic mutations associated with hereditary pancreatitis. Archer et al reported a model relying on the acinar expression of a mutated version of cationic trypsinogen PRSS1,[7] and Durie et al reported cystic fibrosis transmembrane conductance regulator knockout mice.[8] Both mouse models showed somewhat mild pancreatic lesions. Other models have also been described with a variable degree of similarity with human chronic pancreatitis. These are based on defective ciliary function,[9] overexpression of keratin 8,[10] disruption of genes encoding factors associated with the transforming growth factor (TGF)-β signaling pathway,[11] and knockout of PARK,[12] or EIF1 and 2.[13]

An interesting observation in human patients is the variability in individual susceptibility to chronic pancreatitis.[14] This could be related to variability in the immune response, which has been demonstrated to influence the penetrance and severity of chronic inflammatory diseases. Interleukin (IL)-1β is an inflammatory cytokine,[15,16] and polymorphisms in this gene have been shown to affect the immune response.[17] This cytokine has also been shown to have an important role in the pathogenesis of pancreatitis.[18]

We sought to determine whether local activation of the immune system within the pancreas could elicit chronic pancreatitis. We hypothesized that expression of a single proinflammatory cytokine in the pancreas could induce chronic pancreatitis, and, consequently, we created a transgenic mouse, elastase sshIL-1β, in which overexpression of IL-1β is targeted to the pancreas using the elastase promoter.[19] Elastase sshIL-1β mice consistently developed severe chronic pancreatitis that exhibited an early onset and phenocopied well the human disease.

Materials and Methods
Mice

All mice procedures were performed according to the protocol (AC-AAAA5113) approved by the Institutional Animal Use and Care Committee of Columbia University.

The sshIL-1β gene[15,20] was amplified by polymerase chain reaction (PCR), adding *Eco*RI restriction sites at 5′ and 3′ ends. After *Eco*RI digestion, sshIL-1β was inserted downstream the rat elastase promoter (kind gift from Doris Stoffer[19]) and the rabbit β-globin enhancer, and upstream a rabbit β-globin polyA sequence (Figure 1A). Orientation was checked by *Hin*dIII digestion, and the plasmid was sequenced. Elastase sshIL-1β transgene was then extracted from pBluescript by *Xho* and *Xba* digestion and microinjected in the pronucleus of fertilized CBA × C57BL/6J oocytes. Pups were genotyped using 3 different pairs of primers spanning the entire transgene (see supplementary Table 1, genotyping primers, online at www.gastrojournal.org). Positive founders were mated with C57BL/6J mice, and F1 or F2 generations were killed for analysis. Two hours before death, mice were injected with 50 mg/kg BrdU (Sigma–Aldrich, St. Louis, MO) intraperitoneally.

To generate elastase sshIL-1β mice heterozygous for the p53^{R172H} germ-line mutation (elastase sshIL-1β*p53$^{R172H/+}$), elastase sshIL-1β mice (L124) were crossed with mice homozygous for p53^{R172H} mutation (kind gift from Tyler Jacks, Massachusetts Institute of Technology, Cambridge, MA).[21]

For the cerulein-based model of chronic pancreatitis, C57BL/6 mice were injected intraperitoneally with 50 μg/kg cerulein (American Peptide Company, Inc, Sunnyvale, CA; dissolved in sterile water) on 7 consecutive hours, twice a week for 10 weeks, and once a week for 10 additional weeks. Mice were killed 1 week after the last cerulein injection.

Tissue Preparation

For tissue preparations, see Supplementary materials (see Supplementary materials online at www.gastrojournal. org).

Histology, Immunohistochemistry, Immunofluorescence, and Microscopy

For histology, immunohistochemistry, immunofluorescence, and microscopy, see Supplementary materials.

Histologic Analysis and Quantification of Fibrosis

H&E-stained sections were analyzed, and lesions were graded using a modification of the scoring system previously described by Demolset al,[22] taking into account the extent of inflammation, glandular atrophy, and tubular complexes and the percentage of area involved (see supplementary Table 2 online at www.gastrojournal. org). For fibrosis quantification, 6 nonoverlapping ×100 magnification fields of Sirius red stained slides were captured. Morphometric analysis was performed using the IPLab 3.6 software (BD Biosciences, Franklin Lakes, NJ). Preneoplastic lesions were defined according to the criteria of Hruban et al.[23]

Proliferation and Apoptosis Quantification

For proliferation and apoptosis quantification, see Supplementary materials.

Complementary DNA Synthesis and PCR

For complementary DNA (cDNA) synthesis and PCR, see Supplementary materials.

IL Quantification

For IL quantification, see Supplementary materials.

Flow Cytometry

For flow cytometry, see Supplementary materials.

Magnetic Resonance Imaging

For magnetic resonance imaging, see Supplementary materials.

Glucose Tolerance Test

For glucose tolerance test, see Supplementary materials.

Research of Fat Malabsorption

For research of fat malabsorption, see Supplementary materials.

Statistical Analysis

Statistical analysis was performed using t test or Wilcoxon signed-rank test when appropriate, and P values $<.05$ were considered significant. Data are expressed as means $\pm$ SEM.
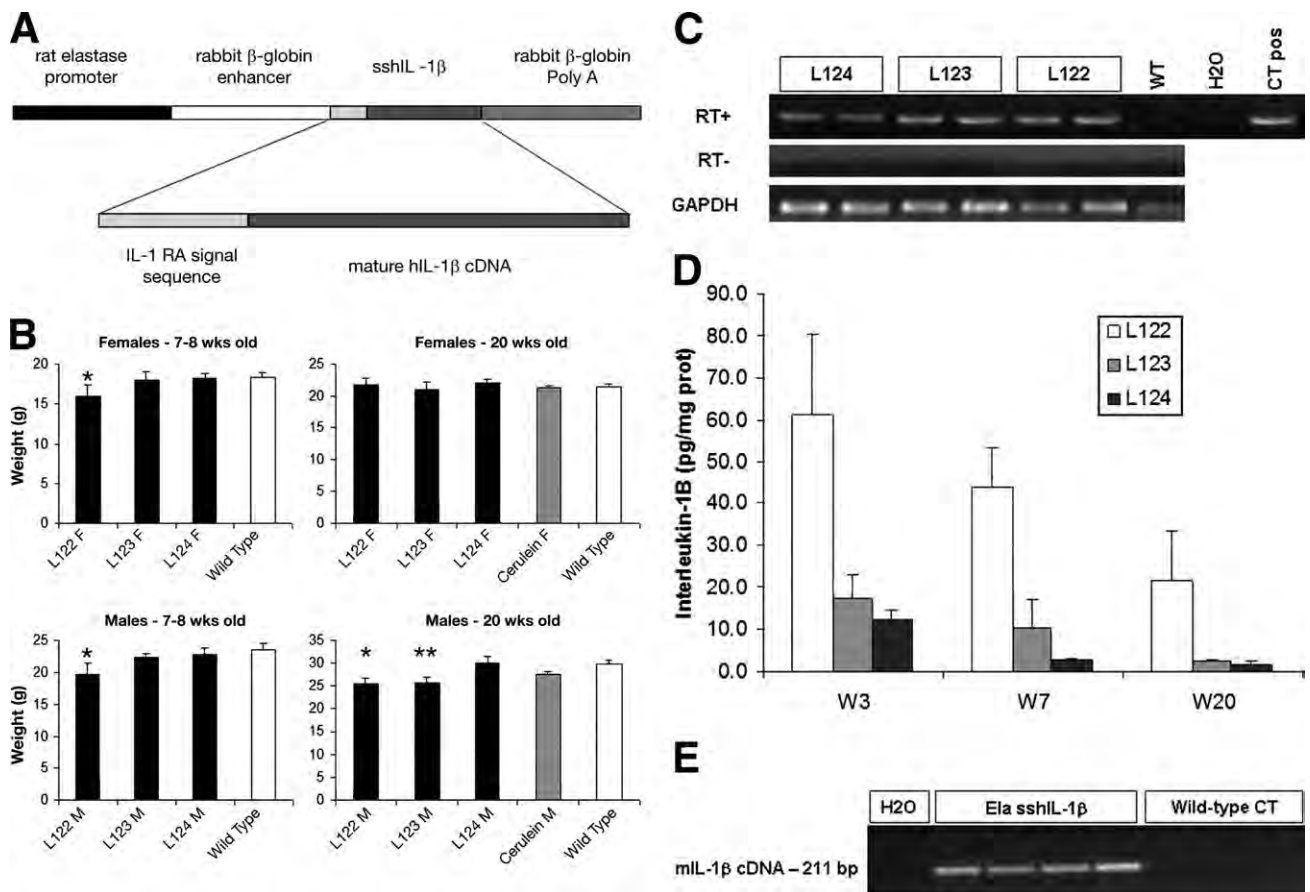

Figure 1. (A) Map of the elastase sshIL-1β construct: the mature human interleukin-1β cDNA was fused with the signal sequence of human interleukin-1 receptor antagonist, allowing secretion without caspase 1 cleavage. Expression of sshIL-1β transgene was driven by the rat elastase promoter. (B) Average weight (error bar is SEM) of elastase sshIL-1β mice, wild-type littermate controls, and cerulein treated mice (20 weeks treatment) (n = 6–22): upper left panel: 7- to 8-week-old females, *P = .01 (/wild-type, t test); upper right panel: 7- to 8-week-old males, *P = .06 (/wild-type); lower left panel: 20-week-old females; lower right panel: 20-week-old males, *P = .00001 (/wild-type), **P = .00005 (/wild-type). (C) Detection of sshIL-1β mRNA in pancreatic tissues of transgenic mice from the 3 different lines. PCR was performed on cDNA isolated from 7- to 8-week-old mice using primers specific for sshIL-1β (forward primer on the sshIL1RA part and reverse primer on the hIL1β part of the transgene). Controls were wild-type littermate (WT) and samples in which reverse transcriptase enzyme had been omitted (RT- line) to control for possible genomic DNA contamination. (D) ELISA quantification of human interleukin-1β in pancreatic protein extracts from 7- to 8-week-old mice from 3 different founders (n = 3–4). Average concentrations of sshIL-1β (error bar is SEM) are reported in pg/mg of pancreatic protein at 3 different ages (3, 7, and 20 weeks old). (E) Murine IL-1β mRNA expression in pancreas of 7-week-old mice detected by RT-PCR. The expected size of the amplified product from tissue cDNA is 211 base pair. Lane 1 (left): negative control. Lanes 2–5: pancreata of elastase sshIL-1β mice (age 7 weeks). Lanes 2 and 3: L122; Lanes 4 and 5: L124. Lanes 6–8: pancreata of wild-type control mice.

Results

### Generation of Elastase sshIL-1β Mice

Three founder mice were generated and subsequently bred to generate 3 separate lines (L122, L123, L124). The litter size was normal for all 3 lines. For lines L122 and L123, approximately 15% of the pups showed significant growth retardation and needed to be killed. The remainder of the elastase sshIL-1β mice displayed normal behavior and growth, although the average weight was significantly lower in L122 mice at 7 weeks and in L122 and L123 male mice at 20 weeks (Figure 1B). For line L124, mice lived up to 2 years, whereas the oldest mice from line 123 are currently 22 months old and appear healthy. Although a detailed survival analysis was not carried out, the elastase sshIL-1β mice do not appear to show any significant decreased longevity compared with wild-type control mice. We confirmed the expression of the sshIL-1β transgene in the pancreas by reverse-transcription (RT)-PCR and by enzyme-linked immunosorbent assay (ELISA) measurement of human IL-1β peptide in pancreatic protein extracts (Figure 1C and D). Expression of sshIL-1β could not be detected in any of the other tissues we analyzed, including liver, submaxillary glands, kidney, lung, and spleen (data not shown). The level of human IL-1β expression was different in the 3 transgenic lines, and these were classified as high (L122), medium (L123), and low (L124) expressers. No human IL-1β was detectable in control mice, which were age matched wild-type mice or mice with cerulein-induced chronic pancreatitis. It is noteworthy that the level of human IL-1β expression decreased with time in all 3 lines, probably related to progressive acinar atrophy as also described in other acinar promoter based transgenic mice.[7] IL-1β itself is a known downstream target of the nuclear factor (NF)-κB pathway. Consistent with the notion that sshIL-1β activates the NF-κB pathway, we could detect strong expression of endogenous murine IL-1β in the pancreata of elastase sshIL-1β mice at the age of 7 weeks, whereas there was only very weak expression in the majority of age-matched, wild-type control mice (Figure 1E). In addition, to demonstrate that human IL-1β can directly activate the murine IL-1 receptor, we isolated myeloid cells from the bone marrow of mice and stimulated these cells with human IL-1β. Treatment of marrow-derived myeloid cells with standard doses of human IL-1β resulted in a >3-fold increase in IL-6 messenger RNA (mRNA) and a >7-fold increase in IL-6 protein secretion (not shown). Because IL-6 is the most commonly used downstream surrogate for IL-1 receptor signaling and NF-κB pathway activation, these findings indicate that human IL-1β can directly stimulate the murine IL-1 receptor.
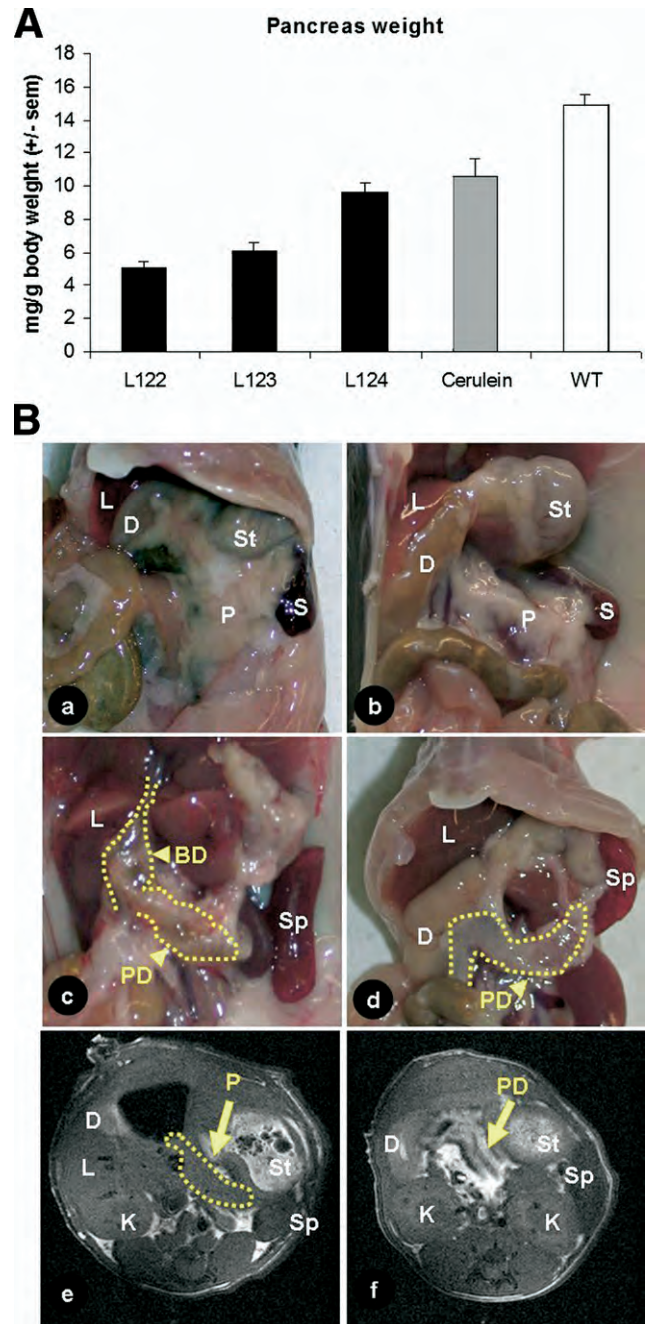
Figure 2. (A) Pancreas to body weight ratio of 7- to 8-week-old elastase sshIL-1β mice, cerulein-treated mice (20 weeks treatment), and wild-type littermate (average ± SEM, n = 4). (B) (a–d) Necropsy of elastase sshIL-1β mice: (a) wild-type littermate; (b) cerulein-treated mice (20-week treatment); (c) elastase sshIL-1β mice: biliary and pancreatic duct dilatation because of fibrosis of the pancreatic head (L123, 11 weeks old); (d) dilatation of the pancreatic duct and atrophic pancreas (L122, 8 weeks old); (e and f): T1 weighted magnetic resonance imaging picture (e) wild-type mouse; the pancreatic duct is not visible; (f) 25-week-old elastase sshIL-1β mouse (L122) displaying a dilated pancreatic duct (arrow). BD, biliary duct; D, duodenum; K, kidney; L, liver; P, pancreas; PD, pancreatic duct; Sp, spleen; St, stomach.

Elastase sshIL-1β Mice Display Chronic Pancreatitis

Pancreata of elastase sshIL-1β mice were atrophic (Figure 2A). In addition, as early as 7 weeks, L122 and
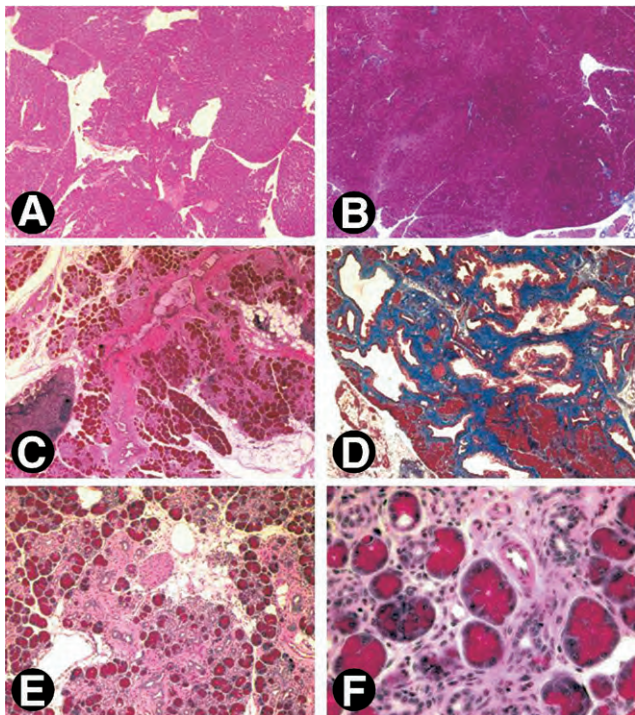
Figure 3. H&E (*A*, *C*, *E*, and *F*) and Masson's trichrome staining (*B* and *D*). Wild-type pancreas (original magnification, ×40; *A* and *B*) and pancreas of 7- to 8-week-old transgenic mice: (*C*) elastase sshIL-1β L124, acinar atrophy, inflammatory infiltrate, and fibrosis surrounding a major duct (original magnification, ×40); (*D*) L122, extensive fibrosis evidenced by Masson's trichrome staining (original magnification, ×40); (*E*) L124, loss of acinar cells, extensive fibrosis, tubular complexes, mixed cellular infiltrate, and increased fat (original magnification, ×100); (*F*) higher magnification (original magnification, ×400): acini and tubular complexes amid mixed inflammatory infiltrate composed of lymphocytes, macrophages, and granulocytes (original magnification, ×400).

L123 mice displayed dilatation of the main pancreatic duct alone, or, in some cases, associated with dilatation of the biliary duct (Figure 2*B*) because of fibrotic stenosis at the level of the head of the pancreas, mimicking human chronic pancreatitis. Histologic analysis showed other features typical of chronic pancreatitis, including acinar atrophy, tubular complexes, mixed inflammatory infiltrate, and fibrosis, the latter confirmed by trichrome staining (Figure 3). These lesions appeared as early as 1 week after birth, starting with a mixed inflammatory infiltrate and initially mild fibrosis. Interestingly, we did not observe pancreatic necrosis at any time point. Complete autopsy did not reveal abnormality in any other organ.

The inflammatory infiltrate consisted mainly of lymphocytes, but variable numbers of macrophages and granulocytes were seen admixed. Characterization of the infiltrate by flow cytometry analysis (Figure 4*A*) demonstrated a predominance of T cells (CD3+) and confirmed the presence of macrophages (CD11b+), granulocytes (gr1+), and B cells (CD19+). The predominance of T lymphocytes was in agreement with the chronic nature of the inflammation.

Increased proliferation and apoptosis in the exocrine pancreas are hallmarks of chronic pancreatitis in humans. We quantified proliferation using immunohistochemical staining for BrdU and apoptosis by the TUNEL assay (Figure 4*B*). Both proliferation and apoptosis were significantly elevated compared with age-matched, wild-type controls.

Chronic pancreatitis is associated with a stromal reaction involving inflammatory cell infiltration as well as proliferation and activation of a specific type of mesenchymal cells called *pancreatic stellate cells*.[24] These cells can be detected by staining for desmin. Figure 5*A* shows increased number of pancreatic stellate cells in elastase sshIL-1β mice, interspersed between acini, located
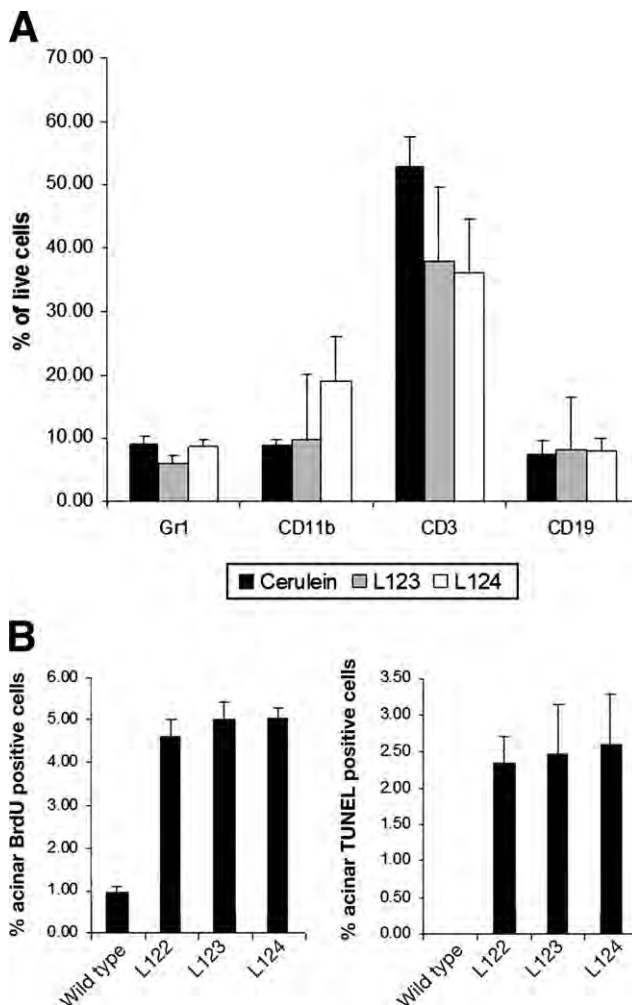

Figure 4. (*A*) Flow cytometry analysis of pancreatic inflammatory infiltrate in 20-week-old elastase sshIL-1β (*L123*, *L124*) and cerulein-treated mice using cell-specific markers: CD3 (T lymphocyte), CD19 (B lymphocyte), Gr1 (granulocyte), and CD11b (macrophage). Results are expressed as average percentage of live cells (*error bar* is SEM) obtained after digestion of pancreatic samples (n = 4). (*B*) Acinar proliferation (BrdU immunohistochemical staining; *left panel*) and apoptosis (TUNEL assay; *right panel*) indexes in 7- to 8-week-old elastase sshIL-1β mice (n = 4). Controls are wild-type littermates. Results are expressed as means; *error bars* are SEM.
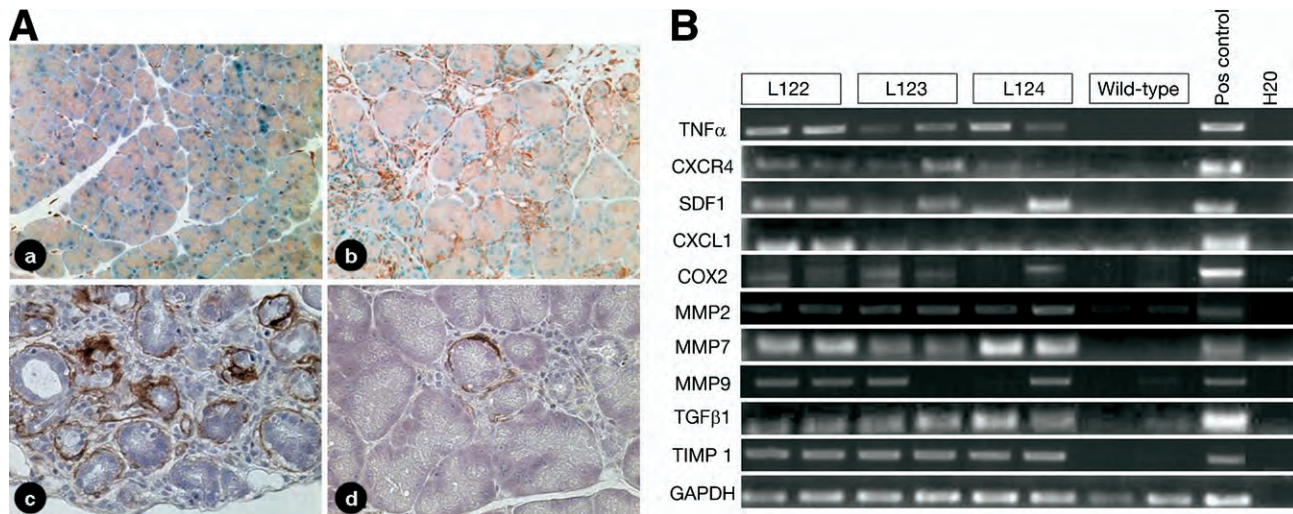
Figure 5. (*A*) (*a* and *b*) Immunohistochemical staining for desmin in 7- to 8-week-old mice: (*a*) wild-type (original magnification, ×40); (*b*) elastase sshIL-1β mouse (original magnification, ×100) pancreatic stellate cells are interspersed between acinar and ductal structures or amid the inflammatory infiltrate. (*c* and *d*) Immunohistochemical staining for α-smooth muscle actin in elastase sshIL-1β mouse: activated pancreatic stellate cells surrounding acini and tubular complexes (original magnification, ×400). (*B*) Reverse-transcription PCR performed on cDNA isolated from 7- to 8-week-old elastase sshIL-1β mice. Controls are wild-type littermates. Transgenic mice show increased mRNA expression of cytokines (*TNF-α*), chemokines (*CXCL1*, *SDF1*, and its receptor chemokine [C-X-C motif] receptor 4), *cyclooxygenase2*, metalloproteases (*MMP2*, *7*, and *9*; *TIMP1*), and *TGF-β1*.

around ducts or regenerative ductules, or scattered amongst the inflammatory infiltrate. Some of these cells, located in the periacinar or periductal area were activated pancreatic stellate cells, as demonstrated by expression of α-smooth muscle actin.

By RT-PCR (Figure 5B), we detected the expression of genes associated with chronic pancreatitis, including TNF-α, which is also a downstream target of IL-1β; chemokines, like stromal cell-derived factor 1 (SDF1) and chemokine (C-X-C motif) ligand 1 (CXCL1); TGF-β1, a
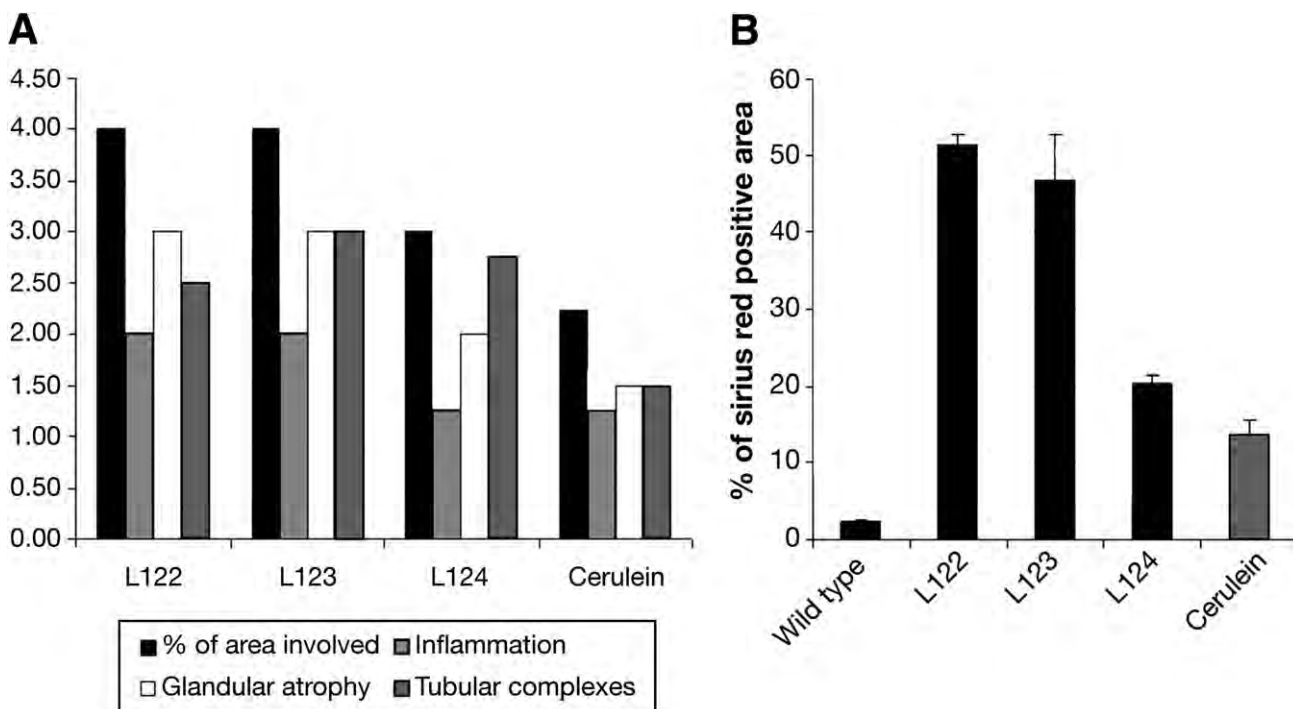
Figure 6. (*A*) Histologic scoring of pancreatic sections based on H&E-stained sections from 20-week-old elastase sshIL-1β mice and wild-type mice treated for 20 weeks with cerulein. Results are expressed as means (n = 4). (*B*) Quantification of collagen area (mean percentage ± SEM) by morphometric analysis after Sirius red staining in the same groups of mice.

growth factor that is involved in pancreatic fibrosis and the activation of pancreatic stellate cells; metalloproteases involved in the remodeling of the extracellular matrix matrix metallopeptidase [MMP] 2, 7, and 9; tissue inhibitor of metalloproteinase [TIMP] 1); and cyclooxygenase 2. These genes all showed minimal expression in the pancreas of wild-type control mice.

Severity of Chronic Pancreatitis Is Correlated With the Expression Level of Human IL-1β

To correlate the extent and severity of the lesions with the level of human IL-1β expression, we graded the lesions and quantified fibrosis by morphometric analysis after Sirius red staining (Figure 6A and B). Mice from lines 122 and 123 (with high and moderate level of sshIL-1β expression, respectively) had more severe lesions and higher levels of fibrosis than mice from the low expressing line (line 124). We also compared the histologic findings in 20-week-old transgenic mice with those of mice treated for 20 weeks with repeated injections of cerulein because the latter has been the most commonly employed model of murine chronic pancreatitis. Despite the protracted protocol, mice that received cerulein had milder lesions and less fibrosis than elastase sshIL-1β mice from any of the 3 lines.

Elastase sshIL-1β Mice Do Not Develop Significant Pancreatic Insufficiency

Severe cases of pancreatitis can be associated with pancreatic endocrine and/or exocrine insufficiency. To assess glucose tolerance in these mice, we performed a glucose tolerance test, which did not demonstrate significant abnormalities of glucose tolerance in transgenic mice compared with wild-type controls (see supplementary Figure 1 online at www.gastrojournal.org). We also evaluated pancreatic exocrine function by assessing for fat malabsorption in mice fed a high fat diet. We performed Oil Red O staining on stool smears (see supplementary Figure 2 online at www.gastrojournal.org) but did not detect any fat in the stools of elastase sshIL-1β mice. It is noteworthy that these tests were performed in mice 8–10 months old to study mice with advanced disease.

Elastase sshIL-1β Mice Develop Acinar-Ductal Metaplasia

Chronic pancreatitis is a well-described risk factor for pancreatic adenocarcinoma. We followed a cohort of transgenic elastase sshIL-1β up to 2 years to determine whether they might develop spontaneous pancreatic neoplasia. Acinar atrophy and fibrosis were progressive, and the majority of the pancreatic gland was replaced over time by adipose tissue. None of the mice developed pancreatic tumors or mouse pancreatic intraepithelial neoplasia (mPanIN). Eosinophilic metaplasia was seen in the large dilated ducts in a few mice, but this lesion is typically considered a reactive change (Figure 7A). We
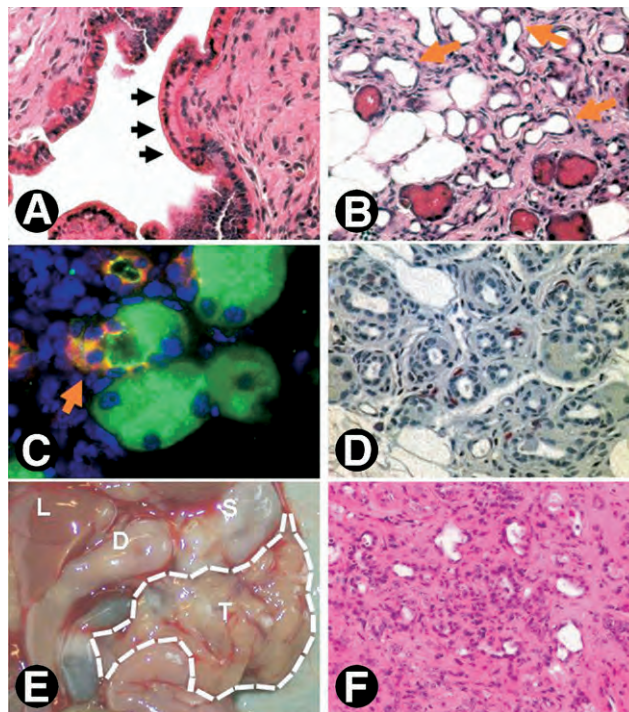

Figure 7. (A) Eosinophilic metaplasia in the main pancreatic duct of an 8-week-old elastase sshIL-1β mouse (L122) (original magnification, ×400); (B) acinar-ductal metaplasia (arrows) in a 20-week-old elastase sshIL-1β mouse (original magnification, ×200); (C) acinar-ductal metaplasia: immunofluorescence for amylase (FITC green) and cytokeratin 19 (Texas Red) showing a cell (arrow) coexpressing both acinar and ductal markers (original magnification, ×900); (D) Representative picture of BrdU immunohistochemical staining in a 20-week-old elastase sshIL-1β mouse showing low epithelial proliferation in tubular complexes (original magnification, ×400); (E) pancreatic tumor in a 43-week-old elastase sshIL-1β*p53$^{R172H/+}$ mouse: T, large nodular tumor replacing the entire pancreas; S, stomach; D, duodenum; L, liver. (F) H&E section of this pancreatic tumor showing sarcomatoid and giant cell differentiation (original magnification, ×200).

also observed acinar-ductal metaplasia starting between 20 (L122 and L123) and 40 weeks of age (L124) (Figure 7B). This lesion was confirmed by performing immunofluorescence staining for amylase and cytokeratin 19 (Figure 7C): in some tubular complexes, cells expressing both acinar and ductal markers were observed. On staining for BrdU (Figure 7D), these lesions had a low proliferation index suggesting acinar transdifferentiation[25] rather than expansion of centroacinar cells as suggested by some studies.[26]

In patients with hereditary chronic pancreatitis, exposure to tobacco, a known mutagen, significantly increases the risk of pancreatic adenocarcinoma.[27] We thus hypothesized that, in addition to chronic inflammation, an additional genetic event might be required to initiate carcinogenesis. Consequently, we crossed elastase sshIL-1β (L124) with mice harboring a R172H mutation in p53[21] and generated elastase sshIL-1β mice heterozygous for p53^{R172H} mutation (elastase sshIL-1β*p53$^{R172H/+}$). These mice had normal growth and development compared

A

B
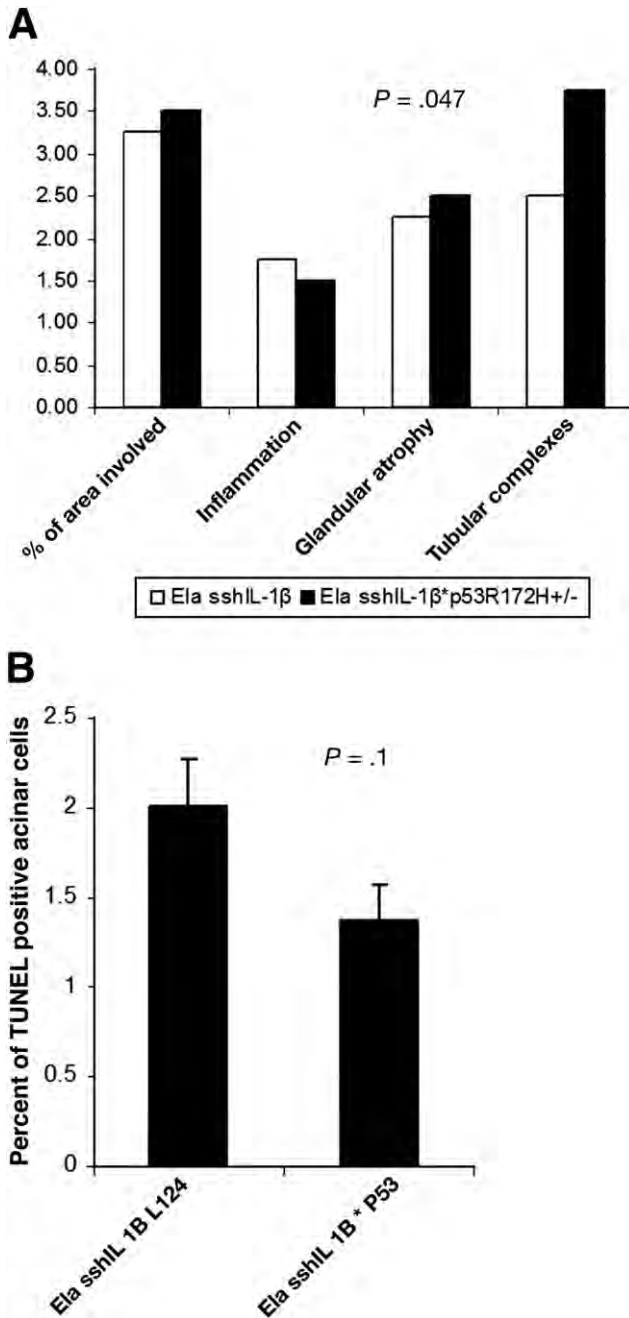
Figure 8. (A) Histologic scoring of pancreatic sections from 40-week-old elastase sshIL-1β*p53$^{R172H/+}$ mice compared with single transgenic elastase sshIL-1β mice from the same founder line (L124), n = 4. Results are shown as means. Extent of tubular complexes is significantly higher in elastase sshIL-1β*p53$^{R172H/+}$ mice (Wilcoxon test). (B) Acinar apoptotic index determined by the TUNEL assay in 40-week-old elastase sshIL-1β mice with or without p53$^{R172H/+}$ mutation. P = 0.1 (t test). Results are shown as means (n = 4); *error bars* are SEM.

with elastase sshIL-1β mice. On comparing the severity of lesions in elastase sshIL-1β mice with or without p53$^{R172H/+}$ mutation, no significant difference in the extent of inflammation or acinar atrophy was observed, but a significantly increased number of tubular complexes, including some showing evidence of acinar-ductal meta-

plasia, was noted in 40-week-old elastase sshIL-1β*p53$^{R172H/+}$ mice (Figure 8A). No difference was observed at 20 weeks old (data not shown). Because p53 is involved in apoptosis regulation,[21] we compared acinar apoptotic indexes according to p53 status and found that elastase sshIL-1β*p53$^{R172H/+}$ mice had a lower apoptotic index, although the difference was not statistically significant (Figure 8B). We did not observe any mPanIN lesion in elastase sshIL-1β*p53$^{R172H/+}$ mice, even in mice up to 15 months of age. Follow-up of this cohort was shorter than that of elastase sshIL-1β mice because, starting at 12 months, mice began to die from p53 germ-line mutation- associated tumors (lymphomas and sarcomas essentially). These tumors occurred with the same frequency as in the single transgenic p53$^{R172H/+}$ control group. Finally, we observed 1 single case of pancreatic tumor (out of 15 mice), an adenocarcinoma with sarcomatoid and giant cell features in a 43-week-old mouse (Figure 7E and F). The pancreas was enlarged and nodular, and the tumor showed extensive invasion with peritoneal carcinomatosis. No liver or lung metastases were identified. In areas of nontumoral pancreas, chronic pancreatitis was evident with acinar-ductal metaplasia, but no mPanIN was observed.

Discussion

Elastase sshIL-1β mice have a phenotype of early onset chronic pancreatitis, with chronic inflammatory infiltrate consisting predominantly of T lymphocytes, progressive glandular atrophy with acinar cell loss, and severe fibrosis, particularly in murine lines with moderate to high levels of human IL-1β expression, leading to biliary and pancreatic duct stenosis. The phenotype was strikingly similar to that of chronic pancreatitis in humans. It was associated with accelerated cellular turnover in the exocrine pancreas and with prominent expression of cytokines (TNF-α), chemokines (CXCL1, SDF1), growth factors (TGF-β1), metalloproteases (MMP2, 7, and 9; TIMP1); and cyclooxygenase 2. Importantly, these mice did not consistently develop pancreatic ductal neoplasm, even in the setting of p53 mutation, but exhibited acinar-ductal metaplasia.

Our results indicate that IL-1β can induce chronic inflammation in the murine pancreas as it has previously been reported in the lung.[16] This conclusion is supported by the fact that all 3 transgenic lines displayed a similar phenotype, which severity correlated with the level of expression of human IL-1β, and by in vitro results showing activation of the IL-1 receptor pathway by human IL-1β. Although sources of IL-1β in human chronic pancreatitis are believed to be leukocytes and stromal cells, we found that targeting hIL-1β expression to acinar cell could consistently induce the disease. As in many transgenic mouse models, overexpression of this proinflammatory cytokine in pancreatic epithelial cells proved to be

effective in replicating human disease but of course does not in any way implicate pancreatic acinar cells as a source of IL-1β production in patients with pancreatitis. Another consequence of the acinar expression of IL-1β could be the induction of an immune response secondary to the expression of the human peptide. Although this appears unlikely, we cannot completely exclude such hypothesis.

Interestingly, some mice with higher levels of human IL-1β expression had a lower body weight, despite the absence of any evidence of fat malabsorption or diabetes. Although decreased body weight has not been reported in other animal models of IL-1β overexpression,[15,16] it is possible that the lower bodyweight was due to the systemic effect of IL-1β as reported by Matsuki et al.[28] Another explanation could possibly be alimentary restriction secondary to the pain associated with food intake.

We did not observe acinar necrosis in the transgenic mice, supporting the concept that the activation of the immune system and of pancreatic stellate cells—in our case resulting from IL-1β activity—is sufficient to induce chronic pancreatitis. This suggests that IL-1β might have a major role in the persistent activation of the immune system leading to chronic pancreatitis. These findings could have important consequences for the understanding and treatment of chronic pancreatitis in humans. For example, polyphormisms in IL-1β gene could influence the penetrance and severity of the disease, and therapy aiming at blocking the action of IL-1β could be considered.

The precise mechanisms of action and direct downstream targets of IL-1β remain unclear. In our model, it appears that overexpression of sshIL-1β led to recruitment and activation of numerous inflammatory cells that further propagated inflammation via secretion of cytokines and chemokines, possibly entailing paracrine and autocrine events. Such view is supported by previous reports of IL-1β function: It has been observed that IL-1β can recruit leukocytes, indirectly, through up regulation of chemokines[16] such as CXCL1 or SDF1, as observed in our mice, or directly, attracting T lymphocytes.[29] This latter cell population is particularly interesting because T lymphocytes can be directly activated by IL-1β,[15] and it has been suggested that T cells could have a direct cytotoxic role in chronic pancreatitis.[30,31] Pancreatic stellate cells are another cell type that could be involved in the response to IL-1β. These cells are known to be involved in the pathogenesis of chronic pancreatitis by synthesizing components and modifiers of the extracellular matrix, contributing to fibrosis, and acting on the microenvironment through paracrine and autocrine mechanisms.[24] Interleukin-1β is a well-described activator of pancreatic stellate cells, and, in agreement, we observed an increase in the number of activated pancreatic stellate cells.

Other murine models of chronic pancreatitis have previously been described. They are based on different mech-

anisms or modes of cellular injury: cerulein administration,[5] genetic engineering,[7-9] chemical injury,[32] or duct ligation.[6] The most widely employed model is the cerulein injection model. However, the model is cumbersome, requiring repeated injections over long periods of time, and results in pancreatic lesions milder than in our model. Chemical and duct ligation models also have limitations in that the lesions tend to decrease over time after the initial injury. More recently, several transgenic models have been described, some of them based on the genetic alterations of hereditary pancreatitis,[7,8] but these models are limited by the low penetrance and significant latency of the phenotype. In this regard, the severity and high penetrance of the phenotype make the elastase sshIL-1β mice a convenient and promising model of chronic pancreatitis.

Chronic pancreatitis is a known risk factor for pancreatic adenocarcinoma.[2,3] Unfortunately, information regarding the mechanistic basis of pancreatic carcinogenesis in the setting of chronic inflammation is scarce, particularly with respect to early genetic events. Recently, it has been reported that cerulein can contribute to pancreatic carcinogenesis in the context of activating KRAS mutation.[33,34] We followed a cohort of transgenic mice for up to 2 years but could not detect any tumors or mPanIN lesions. p53 Mutation is frequent in pancreatic adenocarcinoma,[35] and recent animal models have demonstrated its critical role in neoplastic transformation in the pancreas.[33] Based on these observations, we generated elastase sshIL-1β mice heterozygous for p53^{R172H} mutation.[21] Only 1 mouse developed pancreatic adenocarcinoma at 43 weeks of age. Pancreatic cancer was not observed in our p53^{R172H} controls, but this type of tumor has been reported to occur rarely in mice harboring p53^{R172H} mutation.[21]

We did observe eosinophilic metaplasia and acinar-ductal metaplasia[23] in our double transgenic mice. Eosinophilic metaplasia, which was also seen in our single transgenic mice, has generally been considered a reactive change. The association of acinar-ductal metaplasia with preneoplasia remains the subject of debate, but it is noteworthy that this type of lesion was more extensive in elastase sshIL-1β*p53$^{R172H/+}$ mice. Because p53 mutations have been reported to confer resistance to apoptotic stimuli,[23] it is tempting to speculate that the higher frequency of acinar-ductal metaplasia in elastase sshIL-1β*p53$^{R172H/+}$ mice be the result—as our results suggest—of decreased apoptosis of acinar cells, which subsequently differentiate into ductal cells.

Overall, our results suggest that p53 mutation is not critical for the initiation of carcinogenesis in the setting of chronic pancreatitis, and other molecular pathways may be more relevant. Guerra et al recently reported the effect of cerulein in the setting of activating KRAS mutation.[34] SMAD4 is also a critical antioncogene in pancreatic carcinogenesis[35-39] and is involved in the signal

transduction of TGF-β, which is up regulated in chronic pancreatitis.[32] Future studies are required to investigate the relevance of these pathways for pancreatitis-associated neoplasia.

In conclusion, our results demonstrate that overexpression of IL-1β in the murine pancreas induces chronic pancreatitis, highlighting the potential importance of IL-1β in immune activation in the pancreas. Elastase sshIL-1β mice do not develop spontaneous pancreatic ductal neoplasms but appear to constitute a promising model for studies of chronic pancreatitis and of the role of chronic inflammation in pancreatic carcinogenesis.

Supplementary Data

Note: To access the supplementary material accompanying this article, visit the online version of *Gastroenterology* at www.gastrojournal.org, and at doi: 10.1053/j.gastro.2008.06.078.

References

1. Witt H, Apte MV, Keim V, et al. Chronic pancreatitis: challenges and advances in pathogenesis, genetics, diagnosis, and therapy. Gastroenterology 2007;132:1557–1573.
2. Malka D, Hammel P, Maire F, et al. Risk of pancreatic adenocarcinoma in chronic pancreatitis. Gut 2002;51:849–852.
3. Lowenfels AB, Maisonneuve P, Cavallini G, et al. Pancreatitis and the risk of pancreatic cancer. International Pancreatitis Study Group. N Engl J Med 1993;328:1433–1437.
4. Lowenfels AB, Maisonneuve P, DiMagno EP, et al. Hereditary pancreatitis and the risk of pancreatic cancer. International Hereditary Pancreatitis Study Group. J Natl Cancer Inst 1997;89:442–446.
5. Neuschwander-Tetri BA, Burton FR, Presti ME, et al. Repetitive self-limited acute pancreatitis induces pancreatic fibrogenesis in the mouse. Dig Dis Sci 2000;45:665–674.
6. Watanabe S, Abe K, Anbo Y, et al. Changes in the mouse exocrine pancreas after pancreatic duct ligation: a qualitative and quantitative histological study. Arch Histol Cytol 1995;58:365–374.
7. Archer H, Jura N, Keller J, et al. A mouse model of hereditary pancreatitis generated by transgenic expression of R122H trypsinogen. Gastroenterology 2006;131:1844–1855.
8. Durie PR, Kent G, Phillips MJ, et al. Characteristic multiorgan pathology of cystic fibrosis in a long-living cystic fibrosis transmembrane regulator knockout murine model. Am J Pathol 2004; 164:1481–1493.
9. Cano DA, Sekine S, Hebrok M. Primary cilia deletion in pancreatic epithelial cells results in cyst formation and pancreatitis. Gastroenterology 2006;131:1856–1869.
10. Casanova ML, Bravo A, Ramirez A, et al. Exocrine pancreatic disorders in transgenic mice expressing human keratin 8. J Clin Invest 1999;103:1587–1595.
11. Bottinger EP, Jakubczak JL, Roberts IS, et al. Expression of a dominant-negative mutant TGF-β type II receptor in transgenic mice reveals essential roles for TGF-β in regulation of growth and differentiation in the exocrine pancreas. EMBO J 1997;16:2621–2633.
12. Harding HP, Zeng H, Zhang Y, et al. Diabetes mellitus and exocrine pancreatic dysfunction in perk$^{-/-}$ mice reveals a role for translational control in secretory cell survival. Mol Cell 2001; 7:1153–1163.
13. Iglesias A, Murga M, Laresgoiti U, et al. Diabetes and exocrine pancreatic insufficiency in E2F1/E2F2 double-mutant mice. J Clin Invest 2004;113:1398–1407.
14. Uomo G, Manes G. Risk factors of chronic pancreatitis. Dig Dis 2007;25:282–284.
15. Bjorkdahl O, Akerblad P, Gjorloff-Wingren A, et al. Lymphoid hyperplasia in transgenic mice over-expressing a secreted form of the human interleukin-1β gene product. Immunology 1999;96: 128–137.
16. Lappalainen U, Whitsett JA, Wert SE, et al. Interleukin-1β causes pulmonary inflammation, emphysema, and airway remodeling in the adult murine lung. Am J Respir Cell Mol Biol 2005;32:311–318.
17. Macarthur M, Hold GL, El-Omar EM. Inflammation and cancer II. Role of chronic inflammation and cytokine gene polymorphisms in the pathogenesis of gastrointestinal malignancy. Am J Physiol Gastrointest Liver Physiol 2004;286:G515–G520.
18. Norman JG, Fink GW, Sexton C, et al. Transgenic animals demonstrate a role for the IL-1 receptor in regulating IL-1β gene expression at steady-state and during the systemic stress induced by acute pancreatitis. J Surg Res 1996;63:231–236.
19. Heller RS, Stoffers DA, Bock T, et al. Improved glucose tolerance and acinar dysmorphogenesis by targeted expression of transcription factor PDX-1 to the exocrine pancreas. Diabetes 2001; 50:1553–1561.
20. Wingren AG, Bjorkdahl O, Labuda T, et al. Fusion of a signal sequence to the interleukin-1 β gene directs the protein from cytoplasmic accumulation to extracellular release. Cell Immunol 1996;169:226–237.
21. Olive KP, Tuveson DA, Ruhe ZC, et al. Mutant p53 gain of function in two mouse models of Li-Fraumeni syndrome. Cell 2004;119: 847–860.
22. Demols A, Van Laethem JL, Quertinmont E, et al. Endogenous interleukin-10 modulates fibrosis and regeneration in experimental chronic pancreatitis. Am J Physiol Gastrointest Liver Physiol 2002;282:G1105–G1112.
23. Hruban RH, Adsay NV, Albores-Saavedra J, et al. Pathology of genetically engineered mouse models of pancreatic exocrine cancer: consensus report and recommendations. Cancer Res 2006;66:95–106.
24. Omary MB, Lugea A, Lowe AW, et al. The pancreatic stellate cell: a star on the rise in pancreatic diseases. J Clin Invest 2007;117: 50–59.
25. Means AL, Meszoely IM, Suzuki K, et al. Pancreatic epithelial plasticity mediated by acinar cell transdifferentiation and generation of nestin-positive intermediates. Development 2005;132: 3767–3776.
26. Stanger BZ, Stiles B, Lauwers GY, et al. Pten constrains centroacinar cell expansion and malignant transformation in the pancreas. Cancer Cell 2005;8:185–195.
27. Lowenfels AB, Maisonneuve P, Whitcomb DC, et al. Cigarette smoking as a risk factor for pancreatic cancer in patients with hereditary pancreatitis. JAMA 2001;286:169–170.
28. Matsuki T, Horai R, Sudo K, et al. IL-1 plays an important role in lipid metabolism by regulating insulin levels under physiological conditions. J Exp Med 2003;198:877–888.
29. Hunninghake GW, Glazier AJ, Monick MM, et al. Interleukin-1 is a chemotactic factor for human T-lymphocytes. Am Rev Respir Dis 1987;135:66–71.
30. Demols A, Le Moine O, Desalle F, et al. CD4(+)T cells play an important role in acute experimental pancreatitis in mice. Gastroenterology 2000;118:582–590.
31. Hunger RE, Mueller C, Z'Graggen K, et al. Cytotoxic cells are activated in cellular infiltrates of alcoholic chronic pancreatitis. Gastroenterology 1997;112:1656–1663.
32. Sparmann G, Merkord J, Jaschke A, et al. Pancreatic fibrosis in experimental pancreatitis induced by dibutyltin dichloride. Gastroenterology 1997;112:1664–1672.
33. Hingorani SR, Wang L, Multani AS, et al. Trp53R172H and KrasG12D cooperate to promote chromosomal instability and

widely metastatic pancreatic ductal adenocarcinoma in mice. Cancer Cell 2005;7:469–483.

34. Guerra C, Schuhmacher AJ, Canamero M, et al. Chronic pancreatitis is essential for induction of pancreatic ductal adenocarcinoma by K-Ras oncogenes in adult mice. Cancer Cell 2007;11: 291–302.

35. Tuveson DA, Hingorani SR. Ductal pancreatic cancer in humans and mice. Cold Spring Harb Symp Quant Biol 2005;70:65–72.

36. Bardeesy N, DePinho RA. Pancreatic cancer biology and genetics. Nat Rev Cancer 2002;2:897–909.

37. Izeradjene K, Combs C, Best M, et al. Kras(G12D) and Smad4/ Dpc4 haploinsufficiency cooperate to induce mucinous cystic neoplasms and invasive adenocarcinoma of the pancreas. Cancer Cell 2007;11:229–243.

38. Ijichi H, Chytil A, Gorska AE, et al. Aggressive pancreatic ductal adenocarcinoma in mice caused by pancreas-specific blockade of transforming growth factor-β signaling in cooperation with active Kras expression. Genes Dev 2006;20:3147–3160.

39. Bardeesy N, Cheng KH, Berger JH, et al. Smad4 is dispensable for normal pancreas development yet critical in progression and tumor biology of pancreas cancer. Genes Dev 2006;20:3130–3146.

BASIC–LIVER, PANCREAS, AND BILIARY TRACT

Overexpression of Interleukin-1β in the Murine Pancreas Results in Chronic Pancreatitis

SUPPLEMENTARY MATERIALS

Supplementary Materials and Methods

Tissue Preparation

Pancreata were isolated and washed in cold DEPC water. Portions were cut and snap frozen in liquid nitrogen for protein and RNA extraction. Proteins were extracted using a tissue homogenizer and RIPA buffer + protein inhibitors (complete EDTA free, Roche Applied Science, Indianapolis, IN, USA) and protein quantification was performed using the Bradford method. For RNA isolation, frozen samples were ground using a pestle in liquid nitrogen and homogenized in Trizol reagent (Invitrogen, Carlsbad, CA, USA). RNA was extracted according to manufacturer's instructions and cleaned using RNeasy columns (Qiagen, Valencia, CA, USA). The remaining tissue was fixed overnight in 10% neutral buffered formalin before transfer to 70% ethanol. Specimens were then processed and embedded in paraffin for histologic analysis.

Histology, Immunohistochemistry, Immunofluorescence, Microscopy

Tissue sections (5 μm) were stained with H&E for morphologic analysis Masson's trichrome or Sirius red staining was performed to evaluate the extent of fibrosis.

For immunohistochemical staining, slides were deparaffinized in xylene and endogenous peroxidase was blocked by incubation with 3% hydrogen peroxide in methanol for visualization using the peroxidase reaction. Alternatively, for visualization with the alkaline phosphatase reaction, slides were incubated with 20% acetic acid in methanol for 2 min. Antigen retrieval was performed by boiling the slides in citrate buffer (10mM pH 6.0) in a water bath for 20 min., except for cytokeratin 19 staining, for which incubation with pepsin solution (37°C) for 15 minutes was used for antigen retrieval (Abcam, Cambridge, MA, USA, # ab8194). Slides were rinsed in PBS Tween 0.05% and blocked for 30 min. with 2% bovine serum albumin (Sigma-Aldrich, St. Louis, MO, USA) - PBS. Primary antibodies and biotinylated secondary antibodies (Jackson Immunoresearch, West Grove, PA, USA) were diluted in 2% bovine serum albumin - PBS and incubated for one hour each at room temperature. Subsequently, slides were incubated with alkaline phosphatase or peroxidase conjugated streptavidin (Dako North America, Inc., Carpinteria, CA, USA) and either VectorRed substrate (Vector Laboratories, Burlingame, CA, USA, #SK 5100) or 3,3'-diaminobenzidine (Sigma-Aldrich) as chromogens, respectively. Slides were counterstained with haemtoxylin and mounted for viewing. Primary antibodies used were: BrdU (Abcam, #ab6326, 1/300), α-smooth muscle actin (Dako North America, Inc, M0851, 1/200), desmin (Lab Vision, Fremont, CA, USA, #RB-9014, 1/200), amylase (Sigma-Aldrich, #A8273, 1/500), and cytokeratin 19 (Clone Troma-III developed by Rolf Kelmer was obtained from Development Studies Hybridoma Bank developed under the auspices of the NICHD and

maintained by the University of Iowa, Department of Biological Sciences, 1/25). For primary mouse monoclonal antibodies the ARK kit (Dako North America, Inc) was used according to the manufacturer's instructions.

For immunofluorescence staining, slides were prepared as described above but endogenous peroxidase or alkaline phosphatase blocking was not performed. FITC or Texas Red conjugated secondary antibodies (Jackson Immunoresearch) were utilized. Counterstaining was performed with DAPI (Invitrogen) and slides were mounted in Vectashield mounting medium (Vector Laboratories).

Bright field and fluorescence images were acquired using an Eclipse TU2000-U microscope (Nikon, Melville, NY, USA) connected to a cooled color CCD camera (RTKE Diagnostic Instruments, Sterling Heights, MI, USA) using SPOT software. Confocal fluorescence microscopy was performed using an LSM 510 NLO multiphoton confocal microscope (Zeiss, Thornwood, NY, USA). FITC was excited with a 488 nm argon laser and Texas Red was excited with a 543 nm helium-neon laser. DAPI was imaged using two-photon excitation by a Coherent Mira titanium-sapphire laser (Santa Clara, CA, USA) tuned to 800 nm.

Proliferation and Apoptosis Quantification

Proliferation index was assessed from six non overlapping 400X magnification fields by counting BrdU positive and negative acinar cells. Apoptosis quantification was performed the same way, using the TUNEL assay (ApopTag Plus Peroxidase In Situ Apoptosis Detection Kit, Chemicon, Billerica, MA, USA) according to the manufacturer's instructions.

cDNA Synthesis and Polymerase Chain Reaction

Reverse transcription of mRNA was performed using Superscript First-Strand Synthesis System III (Invitrogen) after digestion with DNase I (Promega, San Luis Obispo, CA, USA) according to the manufacturers' instructions. PCR was performed on cDNA with primer pairs listed in supplementary table 1. Amplification program was as follows: 94°C 2 min., [94°C 30sec.; annealing –see supplementary table 1 for temperatures – 30sec.; extension 72°C 30sec.]x35 but for GAPDH (x30), final extension 72°C-7min..

Interleukins Quantification

To quantify human interleukin-1β in pancreatic tissue, ELISA assays were performed with the Quantikine® Human IL-1β immunoassay (R&D systems, Minneapolis, MN, USA, #DLB50) according to the manufacturer's instructions. Bone marrow myeloid cells secretion of Interleukin 6 was quantified in vitro using the Mouse IL-6 Elisa kit (R&D systems, Minneapolis, MN, USA, #DY406) 24 hours after stimulation with 10 ng/mL human interleukin-1β (BD Biosciences , # 354042).

Flow Cytometry

Small pancreatic samples were harvested and kept on ice before being minced with a blade and digested at 37°C, on a rotating wheel for 25 minutes, with collagenase P 0.05% (Roche Applied Science), pronase 0.02% (Roche Applied Science), and DNAse 0.1% (Roche Applied Science) in Hank's Balanced Salt Solution (Invitrogen)

complemented with bovine serum albumin 0.1% (Sigma) and HEPES 20 mM (Invitrogen). Cells were washed with Hank's Balanced Salt Solution supplemented with 10% fetal bovine serum (Invitrogen) and subsequently with PBS containing 0.5% bovine serum albumin and 1mM EDTA. Immunolabelling was performed after incubation with rat serum (eBioscience, San Diego, CA, USA) using PE-conjugated CD3 and Gr1, and FITC-conjugated CD11b and CD19 (eBioscience). Cells were stained with DAPI to assess viability. Flow cytometry analysis was performed using an LSRII (Becton Dickinson, San Jose, CA, USA) after gating out dead cells.

Magnetic Resonance Imaging

Magnetic Resonance Imaging was performed with a 9.4T magnet and a Bruker Avance 400 spectrometer equipped with a Bruker micro2.5 imaging gradient set with maximum gradient strength of 150 guass/cm. A linear polarized RF birdcage coil insert 3.8 cm in outer diameter, was inserted into the gradient set. There was a 3 cm diameter space in the coil for the animal holder which provided 2.5cm diameter for the animal to be secured for imaging. Two tuning and matching capacitors allowed the RF coil to be tuned to the lamour frequency of 400 MHz. Prior to scanning, mice were anesthetized with 2% isoflourane and a PE-10 size catheter was inserted into the peritoneal cavity. A syringe filled with .7cc of 50 µM gadodiamide (Omniscan) was inserted to the distal side of the catheter. The Magnetic Resonance Imaging scanning protocol consisted of first adjusting the position of the animal in the scanner, with triplanar MSME scout scans, so that the stomach was in the center of the scanning volume (2.1 cm x 2.1 cm x 1.5 cm). Then, shimming was performed and spectrometer parameters were adjusted (5 minutes). A T2 weighted fast spin echo scan was then performed (25 minutes). This was followed by a pre-contrast T1 weighted spin echo scan (15 minutes). The contrast agent gadodiamide was then administered. A series of 3 T1 weighted scans were then performed (each 15 minutes). T2 scans employed echo times of 29.4 ms and repetition times of 1462 ms. T1 scans employed echo times of 7.6 ms and repetition times of 278 ms.

Glucose Tolerance Test

Blood glucose levels were measured, after an overnight fast (baseline) and then 20min., 40min., 60min., and 120 min. after intra-peritoneal injection of glucose 2 mg/g body weight. Blood glucose level was measured using a OneTouch glucometer (LifeScan, Inc., Milpitas, CA, USA).

### Research of Fat Malabsorption

Fat malabsorption was researched by performing Oil Red O staining on stool smears. Groups of 4 mice were fed for three consecutive days with a diet containing 45% fat (Research diet, Inc., New Brunswick, NJ, USA). Stools were then collected over two 6-hour periods on two consecutive days, homogenized in water (10µL/mg stool), and centrifuged for 5 min. at 200g. Five µL of supernatant was applied on a gelatin-coated glass slide and mixed with 5 µL of freshly diluted and filtered Oil Red O. Slides were dried and mounted for viewing.

Supplementary table 1: PCR primers

Primer name	sequence	Length	Annealing Temperature	Comment
mCOX2 F	ggcccttcctcccgtagcaga	449	60	
mCOX2 R	tcatcagaccaggcaccagaccaa			
mTGFβ1 F	acaattcctggcgttacctt	172	50	
mTGFβ1 R	tggagtttgttatctttgctgtca			
mTNFα F	cccaaggcgccacatctcc	575	60	
mTNFα R	ggggcaggggctcttgacg			
mCXCL1 F	ggccccactgcacccaaacc	186	55	
mCXCL1 R	tgttgtcagaagccagcgttcacc			
mSDF1 F	aaaccagtcagcctgagctacc	164	55	
mSDF1 R	aatttcgggtcaatgcacactt			
mCXCR4 F	atggaaccgatcagtgtgag	217	55	
mCXCR4 R	tccttagcttcttctggtaacc			
mTIMP1 F	ccacaatccaacgagaccacc	335	50	
mTIMP1 R	gggatagataaacagggaaacact			
mMMP2 F	ccgggagcgcaacgatgga	495	60	
mMMP2 R	gagaaaagcgcagcggagtgacg			
mMMP7 F	ctttgatgggccagggaacact	144	55	
mMMP7 R	aattcatgggtggcagcaaaca			
mMMP9 F	cgccggcgttcagggagatg	474	55	
mMMP9 R	aagacgaaggggaagacgcacagc			
mGAPDH F	tcaccaccatggagaaggc	168	55	
mGAPDH R	gctaagcagttcgtggtgca			
mIL1 F	ggagaaccaagcaacgacaaaata	211	55	
mIL1 R	tggggaactctgcagactcaaac			
IL1RA- sshIL1β F	ggcctccgcagtcacctaatca	415	57	Genotyping primer
IL1RA- sshIL1β R	tggggaactgggcagactcaaa			
Ela prom - sshIL1β F	acctgtgcttttccctgccttcta	917	57	Genotyping primer
Ela prom - sshIL1β R	ttgttgctccatatcctgtccctg			
sshIL1β polyA F	aatctgtacctgtcctgcgtgttg	476	57	Genotyping primer
sshIL1β polyA R	tcccatatgtccttccgagtgaga			
P53 F	agcctgcctagcttcctcagg	330 (mutated)	57	Genotyping primer
P53 R	cttggagacatagccacactg	290 (wt)		

Supplementary Figures
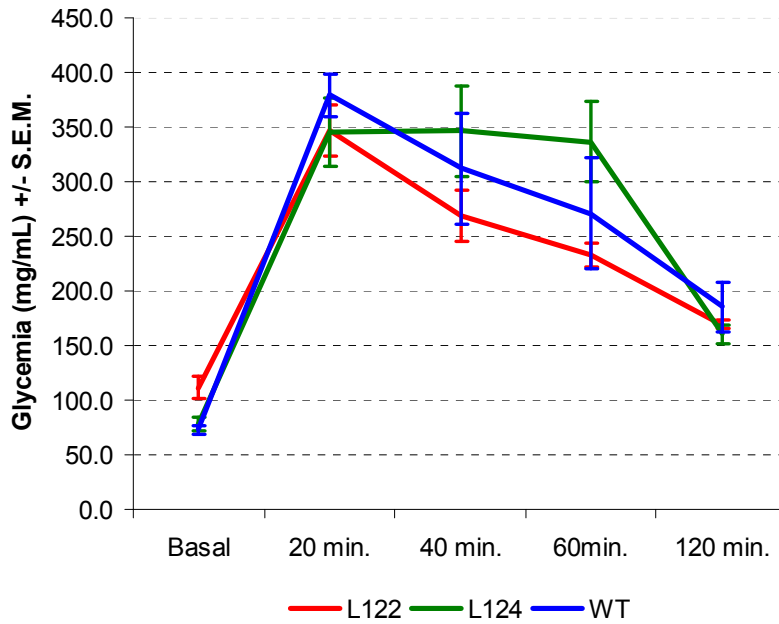
Supplementary Figure 1: Glucose tolerance test in elastase sshIL-1β mice with low (L124) or high (L122) level of interleukin-1β expression, and in wild type littermates. Results are expressed as means (n=5), error bars are S.E.M.
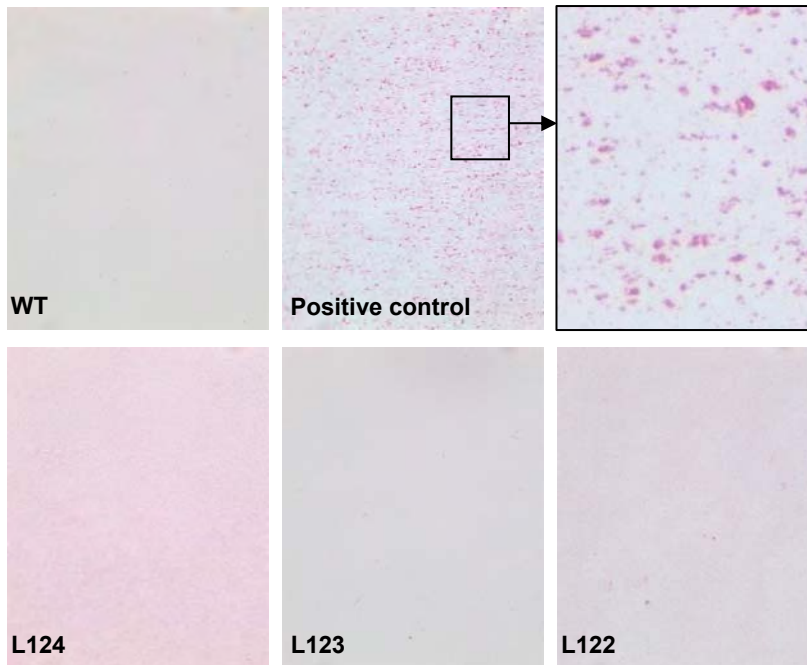
Supplementary Figure 2: Oil Red O staining of stool smears after 48-hour high fat diet in elastase sshIL-1β mice from the three different founder lines (L122-3-4) and wild type littermates (WT). Positive control is ground high fat diet.